



THE UNIVERSITY *of* EDINBURGH

Edinburgh Research Explorer

Tuneable Phosphaamidinate Ligands

Alkyl-Magnesium Complexes Responsive to Increased Ligand Bulk

Citation for published version:

Urwin, SJ, Stanford, MW, Nichol, GS, Garden, JA & Cowley, MJ 2024, 'Tuneable Phosphaamidinate Ligands: Alkyl-Magnesium Complexes Responsive to Increased Ligand Bulk', *European journal of inorganic chemistry*. <https://doi.org/10.1002/ejic.202400735>

Digital Object Identifier (DOI):

[10.1002/ejic.202400735](https://doi.org/10.1002/ejic.202400735)

Link:

[Link to publication record in Edinburgh Research Explorer](#)

Document Version:

Publisher's PDF, also known as Version of record

Published In:

European journal of inorganic chemistry

General rights

Copyright for the publications made accessible via the Edinburgh Research Explorer is retained by the author(s) and / or other copyright owners and it is a condition of accessing these publications that users recognise and abide by the legal requirements associated with these rights.

Take down policy

The University of Edinburgh has made every reasonable effort to ensure that Edinburgh Research Explorer content complies with UK legislation. If you believe that the public display of this file breaches copyright please contact openaccess@ed.ac.uk providing details, and we will remove access to the work immediately and investigate your claim.



Tuneable Phosphaamidinate Ligands: Alkyl-Magnesium Complexes Responsive to Increased Ligand Bulk

Stephanie J. Urwin,^{*,[a]} Martin W. Stanford,^[a] Gary S. Nichol,^[a] Jennifer A. Garden,^{*,[a]} and Michael J. Cowley^{*,[a]}

We describe the synthesis of five new phosphaamidinate ligands of formula RNC(R')P(H)(R''), featuring a hindered tert-butyl-bearing backbone and variable steric bulk at both the nitrogen and phosphorus centres. Crystallographic and heteronuclear NMR studies indicate the geometry of the phosphaamidinate is dependent on the steric bulk of the peripheral substituents, and in one case multiple isomers were observed in solution. Ligand deprotonation by reaction with 0.5 or 1 equivalents of

$n\text{Bu}_2\text{Mg}$ respectively forms heteroleptic (LMg n Bu) or homoleptic (L₂Mg) complexes, with the most bulky phosphaamidinate ligand generating a monomeric, unsolvated three-coordinate magnesium centre. Three LMg n Bu complexes were isolated and show excellent activity for the ring opening polymerization of *rac*-lactide (< 99% conversion in two minutes), with a uniform polymer chain length (\bar{D} = 1.02–1.37).

Introduction

Bidentate nitrogen-donor ligands, such as amidinates and β -diketiminates, are prevalent throughout organometallic chemistry. Their main group metal complexes have diverse applications, and are used as effective bond forming catalysts,^[1] polymerization activators^[2] and molecular reducing agents.^[3] Steric tuning of N-donor ligands including amidinates and β -diketiminates^[4] is a powerful method for manipulating the structures and reactivity of their complexes. Increasing the steric bulk of N-donor substituents has enabled the isolation of two-coordinate Mg(I) systems,^[5] allowed control over the reactions between Mg(I) compounds and carbon monoxide,^[6] and can even be used to enhance the reactivity of Mg(I) systems such that they reduce benzene.^[7] Employed in calcium chemistry, superbulky NacNac ligands even enable the reduction of dinitrogen.^[8]

Steric tuning of N-donor ligands is clearly powerful. In contrast, electronic tuning in these systems has been less widely explored—largely because in much chemistry, the donor properties of the nitrogen centre remain relatively insensitive to the identity of the attached aryl substituent.

In N,N-donors, isoelectronic substitution of one nitrogen atom for phosphorus can at least maintain (and in principle expand) the valuable steric tunability of these ligands. It also

brings additional potential advantages. (i) Phosphorus is larger and more polarizable than nitrogen. The increased accessibility and altered donor strength of the P lone pair may offer access to alternative chemistry; robust Mo and Cr phosphaamidinate complexes have been successfully isolated, whereas the corresponding amidine analogues were unstable.^[9] (ii) Any steric or electronic tuning should be straightforward and 'modular', given the well-developed synthetic chemistry of phosphines. (iii) The ³¹P NMR handle can aid detailed solution state structural studies, as evidenced through the characterization of P,N ligand supported Al complexes.^[10,11]

In spite of the potential benefits of P,N ligands and the extensive use of amidines (RNC(R')N(R'')₂) in main group chemistry, phosphaamidines (RNC(R')P(R'')₂) remain surprisingly underexplored. Only 5 structurally authenticated protic phosphaamidines (RNC(R')P(H)(R'')) and 15 corresponding phosphaamidinate metal complexes have been deposited in the Cambridge Structural Database (Figure S1), with a single example of a magnesium complex. Phosphaamidines can display a phosphinoimine or amino-phosphaalkene structure; in conjunction with E/Z isomerism of the double bond, this results in eight possible structural isomers.^[12] With one exception, reported examples have been isolated as a single isomer in the solid state, with Z-anti(P=C),^[9,12,13] Z-syn(N=C)^[14] and Z-anti(N=C)^[12] structures all represented in the literature (Figure 1A–C). Recently, crystalline (Dipp(H)NC(Tol)P(Dipp)) (**A**) was demonstrated to exist as a mixture of four isomers in CDCl₃ solution. Crystallographic studies of purified **A** indicated a uniform Z-anti(P=C) solid state configuration, however ³¹P CP-MAS solid state NMR analysis of the sample indicated that small amounts of the E-syn(N=C) were also present.^[12]

Complexes featuring an anionic phosphaamidinate can be generated *via* phosphaamidinate deprotonation, silyl abstraction or ligand rearrangement reactions.^[13–19] The serendipitous preparation of the only reported phosphaamidinate magnesium complex **D** resulted from a 1,3-silyl migration.^[17] Phosphaamidinate metal complexes display various coordination modes;

[a] S. J. Urwin, M. W. Stanford, G. S. Nichol, J. A. Garden, M. J. Cowley
School of Chemistry, University of Edinburgh, David Brewster Road,
Edinburgh, EH9 3FJ, UK
E-mail: stephanie.urwin@ed.ac.uk
j.garden@ed.ac.uk
michael.cowley@ed.ac.uk

Supporting information for this article is available on the WWW under
<https://doi.org/10.1002/ejic.202400735>

© 2024 The Author(s). European Journal of Inorganic Chemistry published by Wiley-VCH GmbH. This is an open access article under the terms of the Creative Commons Attribution License, which permits use, distribution and reproduction in any medium, provided the original work is properly cited.

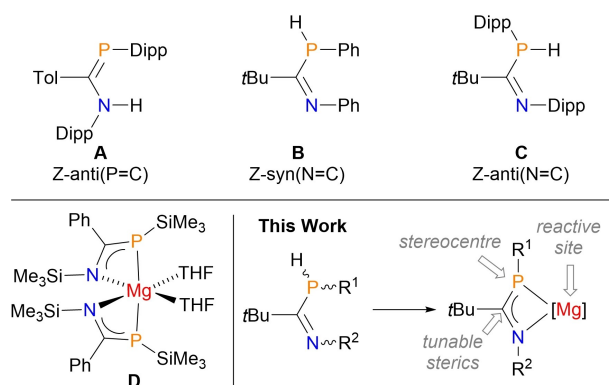


Figure 1. Selected examples of structurally authenticated protic phosphamidines in different geometries (A–C), the only literature example of a phosphoramidate magnesium complex (D), and the new phosphoramidate magnesium complexes reported herein. Tol = *para*-tolyl; Dipp = 2,6-diisopropyl phenyl.

monodentate κN or κP , bidentate N,P chelate, bimetallic bridge and charge-separated ion pair. The delocalization (or otherwise) of the anionic charge across the P–C–N framework surely influences which coordination mode is favoured, though a detailed understanding of precisely how remains unclear and requires further study.

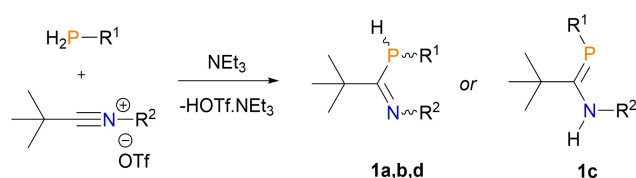
In spite of the potential benefits of P,N ligands compared to their N,N analogues, the catalytic activity of phosphoramidate metal complexes is currently unknown. Here we present the synthesis of five new bulky phosphoramidate ligands and their corresponding homo- and hetero-leptic magnesium complexes, with detailed investigations into their structure and activity towards *rac*-lactide ring-opening polymerization.

Results and Discussion

Phosphoramidate Synthesis

Building on previous studies,^[13,15] a functional group tolerant preparation of phosphoramidates was reported in 2014, combining a carbonitrilium triflate with a primary phosphine in the presence of triethylamine under mild conditions.^[14] Using this method a series of protic phosphoramidates were prepared which varied the size of substituents at both the phosphorus and nitrogen centres. Pro-ligands **1a–d** were prepared in good-to-moderate yield by treatment of the appropriate carbonitrilium triflate salt with the corresponding primary phosphines MesPH₂, TippPH₂ or Mes*PH₂ in the presence of triethylamine (Scheme 1).

The smallest examples in our series, **1a** and **1b**, exist as the phosphinoimine tautomers in both the solid and solution state. Alongside consistent doublet resonances in ¹H and ³¹P NMR spectra (**1a** ¹H δ 4.96, ³¹P δ = –80.6, ¹J_{P–H} = 245 Hz; **1b** ¹H δ 5.03, ³¹P δ –88.9, ¹J_{P–H} = 252 Hz), in ¹³C NMR experiments, **1a** and **1b** exhibit ¹J_{C–P} coupling constants consistent with a C–P single bond (**1a**: ¹³C δ 182.6, ¹J_{C–P} = 59 Hz; **1b**: ¹³C δ 182.7, ¹J_{C–P} = 61 Hz). Single-crystal X-ray studies of **1a** (Figure 2) indicated



Scheme 1. Preparation of novel phosphoramidates **1a–d** from a primary phosphine and carbonitrilium triflate. **1a**: R¹=R²=Mes; **1b**: R¹=Tipp, R²=Mes; **1c**: R¹=Mes*, R²=Mes; **1d**: R¹=Mes, R²<>Dipp. Mes = 2,4,6-trimethyl phenyl, Tipp = 2,4,6-triisopropyl phenyl, Mes* = 2,4,6-tritert-butyl phenyl, Dipp = 2,6-diisopropyl phenyl.

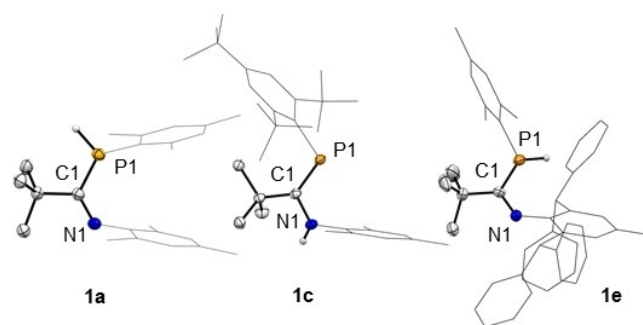


Figure 2. Molecular structures of **1a**, **1c** and **1e**. Hydrogen atoms (except N–H/P–H) omitted and organic substituents wireframe for clarity. Selected bond lengths (Å) **1a**: P1–C3 1.872(3), C3–N1 1.279(4); **1c**: P1–C19 1.7385(17), C19–N1 1.375(6); **1e**: P1–C2 1.8801(18), C2–N1 1.265(2). Selected bond angles (°) **1a**: P1–C3–N1 124.1(2), C17–C3–P1 116.72(19), C17–C3–N1 118.3(2); **1c**: P1–C19–N1 114.32(12), C20–C19–P1 134.83(11), C20–C19–N1 110.84(14); **1e**: P1–C2–N1 118.50(13), C37–C2–P1 123.39(13), C37–C2–N1 117.31(15).

typical C=N double (1.279(4) Å) and C–P single (1.872(3) Å) bond distances. The internal P–C–N angle of **1a** is 124.1(2)°, comparable with those of PhP(H)C(*t*Bu)NPh and CyP(H)C(*t*Bu)NPh (123.16(10)° and 125.22(10)°^[14]) despite the slightly-greater steric bulk of **1a**. A Z-syn(N=C) structure is adopted, presumably a result of the *t*Bu substituent on the central carbon which ‘repels’ the P- and N- substituents. This is further stabilized by parallel-displaced π - π interactions between the aromatic substituents.

In contrast to **1a** and **1b**, Mes* derivative **1c** tautomerizes in solution. In the solid state, **1c** adopts the amino-phosphoramidate tautomer (Figure 2), with short P=C double (1.7385(17) Å) and C–N single (1.375(6) Å) bond distances. In contrast to **1a** and **1b**, **1c** adopts the E-syn(P=C) geometry in the solid state, similar to Boéré and Masuda’s DippP=C(Tol)N(H)Dipp.^[13] Where both P- and N-substituents are bulky, this geometry is seemingly preferred, perhaps because it relieves steric strain. No other solid-state tautomers were found for **1c**.

When crystalline **1c** was dissolved in C₆D₆, ³¹P NMR spectroscopy revealed three signals: δ 98.3 (d, ³J_{P–H} = 18 Hz), δ 80.1 (s) and δ –53.6 (d, ¹J_{P–H} = 253 Hz). Guided by the P–H coupling constants, the two downfield resonances were assigned to phosphoramidate (P=C) tautomers of **1c**, with the high field signal featuring a large *J*_{H–P} arising from a phosphinoimine tautomer. No change to the relative distribution of signals in variable temperature ¹H and ³¹P NMR

spectroscopy indicated that these structural isomers do not interconvert in solution at elevated temperatures, and attempts to fractionally crystallize the remaining two species resulted in sole isolation of the E-syn P=C geometry (*vide supra*).

We investigated which other possible tautomers of **1c** are present in solution using density functional theory (DFT). The eight possible tautomer geometries of **1c** were optimized (M062X/def2svp) and minima were located for seven of the eight possible geometries (**1c-i** to **1c-vii**, numbered in order of increasing energy, Figure S43); a stable minimum was not located for the E-anti(N=C) tautomer. This isomer is thought to be of high energy due to significant steric interactions between the pendant aryl groups and the *t*Bu backbone, and so its omission from the series should not affect our conclusions. Comparison between calculated and experimentally measured geometrical parameters for the E-syn(P=C) tautomer **1c-ii** indicate excellent agreement (e.g. P=C distance 1.7385(17) vs 1.722 Å, Δ = 1.0%; C–N distance 1.375(6) vs 1.387 Å, Δ = 0.2%; P–C–N angle 114.32(12)° vs 114.7° Δ = 0.3%). The relative energy for each of the seven stable tautomers span a range of around 40 kJ mol⁻¹. The solid-state configuration of **1c** was not the lowest energy isomer calculated for the P=C tautomer; the Z-anti(P=C) tautomer **1c-i** was 8.8 kJ mol⁻¹ lower in energy. We therefore assign the two low-field ³¹P NMR signals to these two isomers on the basis that they are the lowest energy Z and E isomers. The Z-syn and E-anti isomers (**1c-iii** and **1c-vii**)–generated by simple rotation about the C–N single bond–are 13.5 and 36.8 kJ mol⁻¹ higher in energy than **1c-i** respectively.

The two ³¹P NMR signals at δ 98.3 (d, ³J_{H-P} = 18 Hz) and δ 80.2 (s) can be assigned specifically to **1c-i** and **1c-ii** on the basis of their H–P coupling constants. Karplus-type arguments rationalizing the magnitude of *J*_{H-P} coupling constants on the basis of the H–P dihedral angle^[20,21] are not applicable here due to a 3-bond distance (*i.e.*, there is no dihedral angle between the atoms of interest). ³J_{H-P} coupling constants are known to correlate with the magnitude of ω, the dihedral angle between the phosphorus lone-pair and the atom to which the hydrogen atom is bonded (in this case: the lone-pair–P–C–N dihedral), such that large dihedral angles result in small H–P coupling constants and vice versa.^[22] The Z-anti isomer **1c-i** has a large ω angle (165.9°) and is thus assigned to the singlet resonance at δ 80.2. ω is small for E-syn **1c-ii** (7.8°) and so the doublet signal at δ 98.3 (³J_{H-P} = 18 Hz) is assigned to it. These assignments are consistent with solution-phase isomerism in **A** (Z-anti(P=C) δ 53.6, s; E-syn(P=C) δ 79.5, d, ³J_{H-P} = 10 Hz).^[12] The remaining signal in the ³¹P NMR spectrum of **1c** at δ –53.6 (¹J_{H-P} = 253 Hz) is assigned to the lowest-energy N=C tautomer, **1c-iv** (Figure 3).

Initial attempts to prepare Ar* substituted phosphamidine **1e** (Ar* = 2,6-bis(diphenylmethyl)-4-methylphenyl) using the same method as for **1a-d** were unsuccessful as the corresponding carbonitrilium salt presented significant handling challenges.^[23] However, treatment of chloroimine Ar*N=C(Cl)*t*Bu with MesPH₂, Me₃SiOTf, and NEt₃ in an analogous one-pot reaction in DCM allowed preparation of **1e** in a low but reproducible yield of 32%; using toluene at high temperature increased the yield of **1e** to 69%. (Scheme 2). Monitoring the reaction using *in situ* ³¹P NMR spectroscopy indicated the

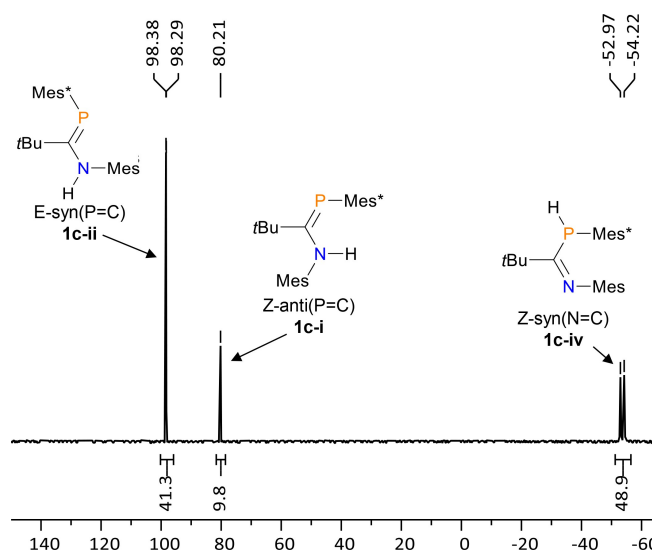
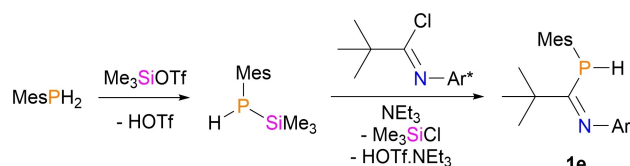


Figure 3. ³¹P NMR spectrum of **1c** (C₆D₆, 202.5 MHz, 300 K), with chemical shifts assigned to isomers present.



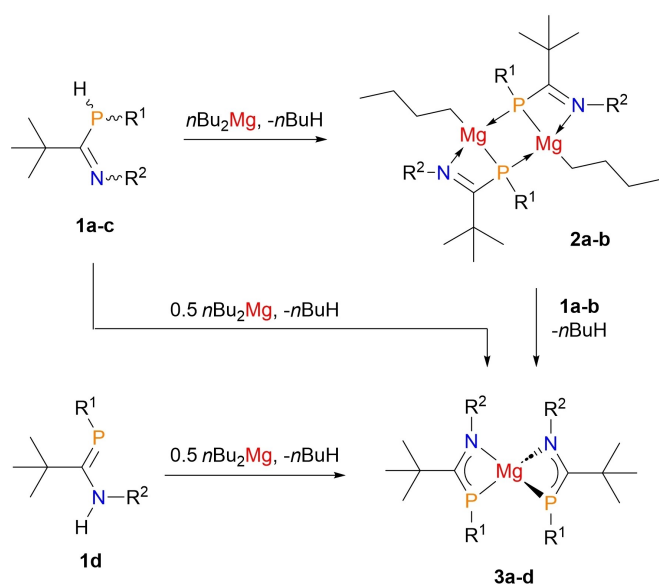
Scheme 2. Preparation of super-bulky phosphamidine **1e**. Ar* = 2,6-bis(diphenylmethyl)-4-methylphenyl.

reaction does not proceed through a carbonitrilium salt, and instead MesP(H)(SiMe₃) forms at room temperature (³¹P δ –160.0 (d, ¹J_{P-H} = 207 Hz)^[24]). When heated to 80 °C this silyl phosphine then reacts with the chloroimine, and the signal of **1e** replaces that of the silyl phosphine. This is reminiscent of the isolation of a tertiary phosphamidine, Ph₂PC(Ph)NPh.^[16] The preparation of silyl phosphines from primary phosphines reacting with trimethylsilyl triflate has been reported for smaller organic groups (Ph and *t*Bu),^[24,25] however larger substituents (Mes, Dipp, Mes*) are usually synthesized by lithiation of the primary phosphine and addition of trimethylsilyl chloride, eliminating lithium chloride in a salt metathesis reaction.^[24,26] **1e** was found to be relatively air- and moisture tolerant; after storing for 2 days in air little degradation had occurred.

Like **1a** and **1b**, super-bulky **1e** exists in solution as the phosphinoimine tautomer, with a ³¹P NMR resonance observed at δ –74.9 (d, ¹J_{H-P} = 249 Hz) and the corresponding proton resonating at δ 5.19 (d, ¹J_{H-P} = 250 Hz) in the ¹H NMR spectrum. Unlike **1a** or **1c**, in the solid state **1e** adopts a Z-anti conformation, which maximizes separation of the mesityl, *t*Bu and Ar* groups. This is confirmed by the single crystal X-ray structure (Figure 2), in which C=N double (1.265(2) Å) and C–P single (1.8801(18) Å) bond distances can be seen. A reduced P–C=N internal angle in **1e** suggests an increase in steric crowding compared to **1a** but on a magnitude comparable to that of **1c** (**1a**: 124.1(2)°; **1c**: 114.32(12)°; **1e**: 118.50(13)°).

Preparation of Magnesium Complexes

The relationship between the steric properties of amidinate ligands and the substitution pattern/nuclearity of the resulting magnesium complexes is firmly established; small amidinate ligands give highly substituted, aggregated complexes,^[27] slightly bulkier amidinate ligands favour heteroleptic complexes which can dimerize^[28,29] and super bulky amidinate ligands produce monomeric compounds.^[30] Treatment of the smallest phosphamidines in our series, **1a** and **1b**, with 1 equivalent of $n\text{Bu}_2\text{Mg}$ forms the $\text{LMg}n\text{Bu}$ complexes **2a** and **2b**, by elimination of butane (Scheme 3). In both cases, an immediate colour change from colourless to bright yellow accompanies a new singlet signal in the ^{31}P NMR spectrum (**2a**: $\delta -41.9$; **2b**: $\delta -55.3$). The loss of P–H resonances is also evident in the



Scheme 3. Preparation of magnesium complexes discussed. **1-3 a**: $\text{R}^1=\text{R}^2=\text{Mes}$; **1-3 b**: $\text{R}^1=\text{Tipp}$, $\text{R}^2=\text{Mes}$; **1-3 c**: $\text{R}^1=\text{Mes}^*$, $\text{R}^2=\text{Mes}$; **1,3 d**: $\text{R}^1=\text{Mes}$, $\text{R}^2=\text{Dipp}$.

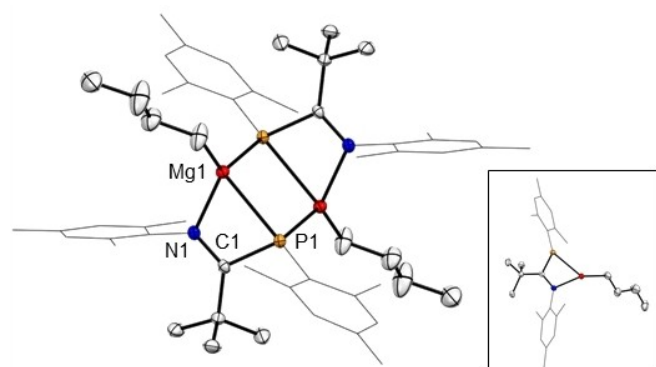


Figure 4. Molecular structure of **2a** with the asymmetric unit shown inset. Hydrogen atoms are omitted for clarity. Selected bond lengths (Å): P2–Mg1 2.6185(8), P1–Mg2 2.6186(8), (Å): Mg1–P1 2.5937(8), P1–C5 1.8527(19), C5–N1 1.303(3), N1–Mg1 2.1717(17). Selected bond angles (°): P1–C5–N1 108.03(13), C5–N1–C19 127.66(16), C5–P1–C10 111.93(9), P1–Mg1–N1 64.65(3).

corresponding ^1H NMR spectra. A series of multiplet signals corresponding to the $n\text{Bu}$ groups are observed, including distinctive signals arising from the AA'XX' spin system of the LMgCH_2 groups at δ 0.49 (Figure S16).^[31] In the ^{13}C NMR spectrum of **2a**, the signal for the central carbon atom of the phosphamidinate ligand is significantly downfield from that in the phosphamidine (**1a**: δ 182.5, d, $^1J_{\text{C-P}}=59$ Hz; **2a**: δ 211.2 (d, $^1J_{\text{C-P}}=14$ Hz)). A decrease in C–P coupling constant indicates metal coordination to phosphorus^[32] (**2a**: 14 Hz, **1a**: 59 Hz; **2b**: 15 Hz, **1b**: 61 Hz).

The structures of **2a** and **2b**, determined by single-crystal X-ray diffraction, reveal dimeric structures in the solid-state (Figure 4). Due to the 1,3-coordination mode of the phosphamidinate ligand, the conformations of the free phosphamidines are not maintained on deprotonation and complexation to Mg. Intermolecular coordination of the phosphorus lone pairs results in 4-coordinate magnesium centres, with dative Mg–P interactions taking the place of the coordinated solvent that is commonly observed in magnesium alkyl complexes. The tetrahedral geometry at phosphorus gives **2a** and **2b** a stereogenic centre, though both compounds exist as racemic mixtures. In the solid state, a centre of inversion located within the Mg_2P_2 ring means the dimeric structures are *meso* compounds.

Upon coordination to magnesium, the backbone P–C bond distance of **1a** contracts marginally (1.872(3) Å to 1.8527(19) Å) whereas the C–N bond lengthens (1.279(4) Å to 1.303(3) Å), with bond distances in **2a** leading to the conclusion of an overall phosphide-imine structure. This lack of delocalization of the anionic charge across P and N centres is in contrast to previous observations with phosphamidinate lithium complexes (*cf.* [DippNC(Tol)Pdipp][Li]: P–C 1.766(2) Å, C–N 1.343(3) Å; [DippNC(*t*Bu)Pdipp][Li]: P–C 1.796(3) Å, C–N 1.317(3) Å).^[13,15] This is likely a result of coordination of two magnesium centres to each phosphorus acting as a superior sink for the negative charge than conjugation with the C=N bond. The increase in steric bulk of our phosphamidinate ligand compared to literature analogues is reflected in the N–C–P bite-angle, which is narrower in **2a** than in the previously reported lithium complex with a sterically demanding phosphamidinate ligand bonding (**2a**: 108.03(13)°; [PhNC(*t*Bu)P(Mes*)]Li(THF)₂: 122.34(16)°, κN coordination^[14]). It is noted that Mg1–P1 and Mg1–P2 bond lengths in **2a** are very similar at 2.5937(8) Å and 2.6186(8) Å. The solid-state molecular structure of **2b** is largely identical to that of **2a** (Figure S42). Comparison of the P–Mg–N bite-angles and percentage buried volume ($\%V_{\text{bur}}$)^[33] suggests that the metal centre in Tipp-substituted **2b** is not significantly more sterically crowded than in **2a** (**2a**: P–Mg–N = 64.65(3)°, $\%V_{\text{bur}}=38.8\%$; **2b**: P–Mg–N = 64.51(4)°, $\%V_{\text{bur}}=40.7\%$. $\%V_{\text{bur}}$ calculated without $n\text{Bu}$ group).

When the Mes*-substituted phosphamidine **1c**, the bulkiest of our series at phosphorus, was treated with 1 equivalent of $n\text{Bu}_2\text{Mg}$, ^{31}P NMR spectroscopy revealed, in addition to substantial amounts of unreacted **1c**, a new singlet signal at δ 12.5 that is distinctly different from those observed for the parent ligand **1c** (^{31}P δ 98.4, 80.2 and 53.6) or $\text{LMg}n\text{Bu}$ complexes **2a** (^{31}P δ –41.9) and **2b** (^{31}P δ –55.3). In the

corresponding ^1H NMR spectrum, no signals attributable to $n\text{Bu}$ groups were observed. When **1c**, which exists in solution as a mixture of one phosphino-imine and two phosphalkene tautomers, is reacted in a 2:1 ratio with $n\text{Bu}_2\text{Mg}$ the same product is observed by NMR spectroscopy, only this time with complete consumption of **1c**. The observed stoichiometry and spectroscopic observations are consistent with the formation of the L_2Mg type complex **3c**, which was confirmed by single-crystal X-ray diffraction studies (Figure 5). The solid state structure of **3c** confirms a distorted tetrahedral magnesium centre (bond angle range = $66.20(4)^\circ$ – $140.38(3)^\circ$) coordinated by two phosphoramidate ligands. The distorted geometry at magnesium results from the narrow bite-angle of the two phosphoramidate ligands. The P–C bond distance is the shortest of the phosphamidate complexes reported here, at $1.7946(16)$ Å, and the C–N distance is $1.334(2)$ Å, longer than a C=N double bond (*ca.* 1.27 – 1.30 Å) and in-range for a delocalized imine (*ca.* 1.33 – 1.41 Å).^[34] As sp^2 hybridization is maintained around C1 ($\Sigma_{\text{C1}} = 359.24(13)^\circ$; $\Sigma_{\text{C33}} = 359.39(12)^\circ$), we conclude that the anionic charge of the ligand is delocalized to a greater degree across the phosphorus and nitrogen centres than in the $\text{LMg}n\text{Bu}$ complexes **2a** and **2b**.

The L_2Mg complexes **3a** and **3b**, derived from the smaller phosphoramidate ligands **1a** and **1b** can also be prepared by treating the phosphoramidates with 0.5 equivalents of $n\text{Bu}_2\text{Mg}$. We made no crystallographic study of these compounds but characterized them spectroscopically. Both compounds contain only one ligand environment, and resonate as singlets in their ^{31}P NMR spectra at $\delta -25.9$ (**3a**) and $\delta -34.3$ (**3b**). In the ^{13}C NMR spectrum, and consistent with all phosphoramidate complexes described here, the central carbon of the ligand gives rise to doublet signals for **3a** at $\delta 222.6$ (d, $^1J_{\text{C-P}} = 60$ Hz) and for **3b** at $\delta 211.30$ (d, $^1J_{\text{C-P}} = 58$ Hz). Treatment of the L_2Mg complex **3a** with 1 equivalent of $n\text{Bu}_2\text{Mg}$ results in formation of

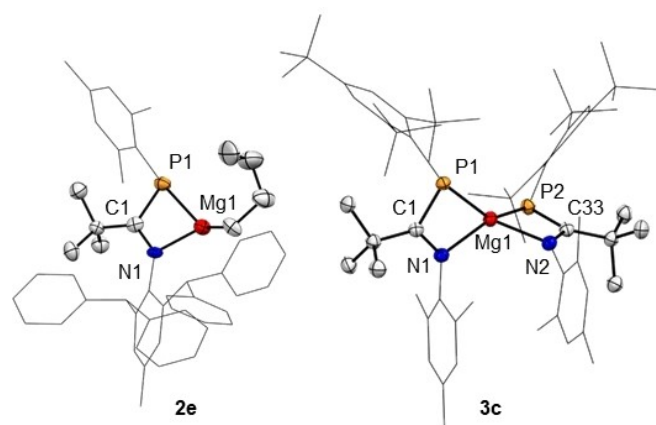


Figure 5. Molecular structures of **2e** (asymmetric unit) and **3c**. Hydrogen atoms omitted and organic substituents are wireframe for clarity. Only one position of the disordered $n\text{Bu}$ group is represented in **2e**. $2\text{C}_6\text{D}_6$ of crystallization in **3c** are omitted for clarity. Selected bond lengths in **3c** (Å): P1–C1 $1.7883(17)$, P1–Mg1 $2.5093(6)$, C1–N1 $1.334(2)$, N1–Mg1 $2.0930(15)$, P2–C33 $1.7946(16)$, P2–Mg1 $2.5064(7)$, N2–C33 $1.334(2)$, N2–Mg1 $2.0977(14)$. Selected bond angles in **3c** ($^\circ$): P1–C1–N1 $107.81(12)$, P2–C33–N2 $107.84(11)$, P1–Mg1–N1 $66.20(4)$, P2–Mg1–N2 $66.7(4)$, P1–Mg1–P2 $140.38(3)$, N1–Mg–N2 $119.94(6)$.

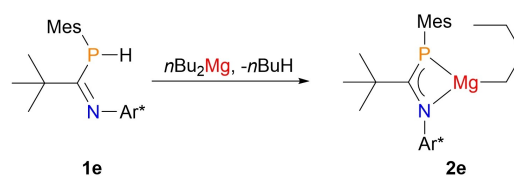
the $\text{LMg}n\text{Bu}$ complex **2a**, whilst **3a** can also be prepared from **2a** and one equivalent of **1a**.

Next, we examined the ligand **1d**, which bears a Dipp substituent at the nitrogen centre. Treatment of **1d** with one equivalent of $n\text{Bu}_2\text{Mg}$ forms an inseparable mixture of the heteroleptic complex **2d** and homoleptic **3d**, the latter of which is the major product, as determined on the basis of resonances in the ^{31}P NMR spectrum at $\delta -44.8$ (**2d**) and $\delta -20.5$ (**3d**). Comparison of the chemical shift for **2d** with others in our series reveals that heteroleptic **2d** is likely a dimer in solution, with a structure comparable to **2a** and **2b**. When **1d** is treated with 0.5 equivalents of $n\text{Bu}_2\text{Mg}$, a mixture of **2d** and **3d** is formed. Using sub-stoichiometric $n\text{Bu}_2\text{Mg}$ enables the isolation of **3d**, albeit in a low yield (57%) and with trace contamination of **2d** remaining.

The super-bulky phosphoramidate ligand **1e** reacts sluggishly with one equivalent of $n\text{Bu}_2\text{Mg}$ at room temperature, however heating the mixture to 90°C for 12 hours results in a colour change and formation of the heteroleptic $\text{LMg}n\text{Bu}$ complex **2e** (Scheme 4). In the ^{31}P NMR spectrum, a singlet signal at $\delta -7.03$ is observed, and the ^1H NMR spectrum has resonances corresponding to a $\text{Mg}n\text{Bu}$ group, including a broad high-field signal at $\delta = -0.56$ – 0.73 for the MgCH_2 protons. No reaction was observed with further equivalents of **1e** even under forcing conditions, *i.e.*, it was not possible to form an L_2Mg complex using this super-bulky phosphoramidate.

Compound **2e** was isolated in 78% yield. Single crystal X-ray diffraction experiments revealed that, unlike **2a** and **2b**, **2e** is monomeric in the solid state and contains an unsolvated, three-coordinate magnesium centre (Figure 5), similar to a β -diketiminato supported example derived from the same super-bulky amine.^[30] Although three-coordinate monomeric magnesium complexes can be readily prepared with more sterically demanding alkyl groups such as isopropyl^[35] or $t\text{Bu}$,^[36] examples bearing an $n\text{Bu}$ group are rare. Although the diffraction data from **2e** was of sufficient quality to assist in formulation of the compound, it proved insufficient to enable accurate determination or discussion of bond metrics. The three-coordinate phosphorus centre of **2e** is stereogenic, however the compound crystallizes as a racemic mixture.

Whilst there is substantial disorder around the pendant n -butyl ligand, it clearly adopts an unusual ‘folded back’ conformation, which we believe is enforced by the large steric bulk of the nitrogen substituent. The steric crowding is reflected in a $\%V_{\text{bur}}$ value of 58.9%, much greater than the values for **2a** (38.8%) or **2b** (40.7%). Given the shift in ^{31}P NMR resonance of **2e** ($\delta -7.03$) is substantially downfield compared to dimeric **2a**

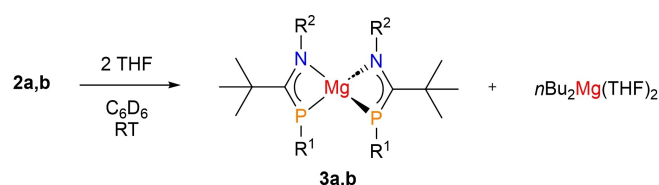


Scheme 4. Preparation of a monomeric, three-coordinate magnesium. $\text{Ar}^* = 2,6$ -bis(diphenylmethyl)-4-methylphenyl.

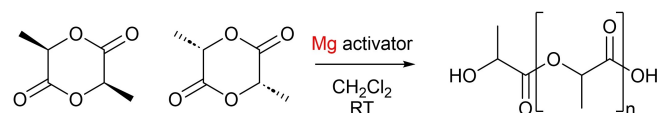
(δ –41.9) and **2b** (δ –55.3), we conclude that **2e** remains monomeric in solution.

Ring-opening Polymerization Studies

Several N,N-ligated Mg complexes have shown excellent activity in the ring-opening polymerization (ROP) of *racemic*-lactide (*rac*-LA) to poly(lactic acid) (PLA), including those based on β -diketiminato, heteroscorpionate and aza-(oxazoline) ligands.^[31,37–39] As PLA can be used in biomedical applications,^[40] magnesium-based catalysts are attractive due to the low toxicity, lack of colour and low cost of this metal. Heteroleptic **2a**, **2b** and **2e** were therefore tested for *rac*-LA ROP. Each of these complexes bears a *n*-butyl group as a single-site initiator



Scheme 5. Reaction of magnesium complexes **2a** and **2b** with stoichiometric THF in C_6D_6 .



Scheme 6. Ring-opening polymerization of *rac*-lactide to poly(lactic acid), initiated by phosphoramidinate magnesium complexes. Mg activator = **2a**, **2b** or **2e**.

for controlled chain growth, similar to N,N-ligated Mg-alkyl complexes previously reported for cyclic ester ROP.^[31,37] The polymerization conditions selected are commonly used in testing Mg complexes as catalysts for *rac*-LA ROP (Scheme 6; [LA] = 1.0 M, with 1 [Mg] mol% or 0.5 [Mg] mol% catalyst loading ([Mg] vs LA) in dichloromethane solution at 20 °C).^[31,39,41] While THF solvent has been used with other Mg complexes for *rac*-LA ROP,^[42,43] ³¹P NMR studies showed that the stoichiometric addition of Lewis donor THF resulted in the formation of the bis-ligated Mg species through the Schlenk equilibrium. This was identified by a downfield shift of the ³¹P NMR resonance (from δ = –42.0 to δ = –22.2 for **2a**, and from δ = –55.3 to δ = –34.1 for **2b**), corresponding to the formation of **3a** and **3b**, respectively (Scheme 5). As the formation of L_2Mg complexes has been reported as a catalyst deactivation pathway within amidinate chemistry,^[29] dichloromethane was thus selected as the solvent for ROP studies using **2a**, **2b** and **2e** as initiators (Scheme 6). Representative NMR studies confirmed that **2a** and **2b** persist in DCM solutions under the polymerisation conditions (Figures S36 and S37).

Complexes **2a**, **2b** and **2e** all display high catalytic activities for the polymerization of LA (Table 1). At 1 mol% [Mg] loading (vs [LA]), all three catalysts display relatively similar activities although catalyst **2a** displayed slightly lower activities than the bulkier **2b** analogue (Entries 1 and 3). The lower activity of the less sterically bulky **2a** catalyst falls in line with previously reported trends within magnesium catalysts for the ROP of LA.^[37,45] All three catalysts remained active at lower catalyst loadings (0.5 [Mg] mol%, Entries 6–9), with **2b** appearing to be the most robust system, achieving 98% conversion of LA in 5 minutes (Entry 7). In general, **2a** delivered the lowest dispersity (\mathcal{D}) values (e.g. \mathcal{D} = 1.06 at 0.5 [Mg] mol% catalyst loading, Entry 6) in the absence of further additives. Alcohols

Table 1. Polymerizations of *rac*-lactide catalysed by **2a**, **2b** and **2e**.

	[Mg] ^[a] (mol%)	MeOH (mol%)	Time (min)	Conv ^[b] (%)	M_n ^[c] (Da)	$M_{n,calc}$ ^[d] (Da)	\mathcal{D} ^[c]
1	2a [1.0]	–	1 ^[e]	46	–	–	–
2	2a [1.0]	–	30	98	5690	14110	1.13
3	2b [1.0]	–	1 ^[e]	98	–	–	–
4	2b [1.0]	–	30	98	7870	14110	1.26
5	2e [1.0]	–	2	99	15540	14260	1.37
6	2a [0.5]	–	30	87	4260	25060	1.06
7	2b [0.5]	–	5	98	–	–	–
8	2b [0.5]	–	30	98	7840	28220	1.08
9	2e [0.5]	–	5	70	14370	20160	1.28
10	2a [1.0]	1.0	3 ^[e]	5	–	–	–
11	2a [1.0]	1.0	30	10	–	–	–
12	2b [1.0]	1.0	3 ^[e]	19	–	–	–
13	2b [1.0]	1.0	30	91	3800	13110	1.02
14	2e [1.0]	1.0	2	98	7720	14110	1.16
15	3a [10]	–	60	20	–	–	–

Reaction conditions: dichloromethane, [LA] = 1.0 M. ^[a] concentration relative to number of magnesium centres. ^[b] Determined by ¹H NMR. ^[c] Determined by size-exclusion chromatography analysis in THF, using a triple detection system and using a dn/dc value of 0.05 mL/g for poly(lactic acid).^[44] ^[d] Calculated from the monomer conversion $M_{n,calc} = M_0 \times ([M]/[I]) \times \text{conversion}$ assuming 1 chain per catalyst. ^[e] 0.1 mL reaction aliquot quenched in excess hexane.

can be added to cyclic ester ring-opening polymerizations as a method of controlling the molar mass and decreasing the dispersity.^[46] Here, the addition of 1 equivalent of methanol to the most sterically hindered catalyst **2e** improved the dispersity from 1.37 to 1.16 (Entries 5 and 14). However, the addition of methanol significantly decreased the catalytic activity of **2a**, giving just 10% conversion after 30 minutes. The polymerizations were moderately well-controlled, with catalyst **2b** giving a dispersity of 1.02 at 91% conversion (Entry 13), albeit with **2a** and **2b** giving lower than expected $M_{n,obs}$ values. In contrast, **2e** generally gives good agreement between the $M_{n,obs}$ and $M_{n,calc}$ values (Entry 5). This difference may arise from the structural differences between monomeric **2e** and dimeric **2a-2b**. Catalysts **2a**, **2b** and **2e** are comparable with the most active magnesium catalysts reported for the ROP of LA,^[31,39,47] including a diketimate complex, $[\text{CH}(\text{CMe})(2,6\text{-}i\text{Pr}_2\text{C}_6\text{H}_3\text{N})_2\text{Mg}(\text{O}i\text{Pr})]$, which gave 97% conversion of LA to PLA in two minutes (dichloromethane solvent, 20 °C, 1 mol% catalyst loading, 1 equivalent of $i\text{PrOH}$).^[41] A comparable polymerization experiment using homoleptic **3a** as an initiator gave only trace conversion of *rac*-LA to PLA after 18 hours of reaction time.

Microstructural analysis of the PLA by decoupled ¹H NMR spectroscopy revealed that sterically encumbered **2b** gave PLA with a very slight isotactic preference (**2b**, $P_i=0.55$), whereas **2a** and **2e** yielded essentially atactic PLA ($P_i=0.48$ and 0.52, respectively).^[48] This lack of stereocontrol was expected from meso **2a/2b** and racemic **2e**, and is in line with previous reports of magnesium catalysts for the ROP of LA, which are generally highly active but not very stereoselective.^[35,41,49]

MALDI-ToF analysis is an established method of identifying polymer chain end-groups.^[50] Here, the MALDI-ToF analysis of the purified polymers prepared using **2a** shows the presence of α -butyl- ω -hydroxyl end-capped PLA, as well as a telechelic polymer terminated by hydroxyl groups (Figure S41). This aligns with previous reports of related magnesium-*n*-butyl catalysts for LA ROP.^[31,37,39,51,52] In the presence of one catalytic equivalent of MeOH, evidence of chain transfer was observed with α -methoxy- ω -hydroxyl PLA present, in addition to the di-hydroxyl terminated polymer and macrocyclic PLA; this was further corroborated by the lower $M_{n,obs}$ values (cf. the $M_{n,calc}$ values, Entries 4–5 vs 13–14).^[53] To provide further support for the presence of *n*Bu end groups and to probe the nature of the active species, we investigated the NMR scale reaction of **2a** with LA in C_6D_6 solvent (selected to allow comparison with **2a**, Figure S16). Upon the addition of two equivalents of LA per **2a** dimer, a new broad ³¹P NMR resonance was observed at $\delta=13.9$, alongside **1a** as a minor product (Figure S37), suggesting that the phosphorous environment has changed from four-coordinate to three-coordinate (cf. three-coordinate **2e**: $\delta=-7.0$). The concurrent disappearance of the AA'XX' ¹H NMR resonance, corresponding to the MgCH_2 group, upon reaction of **2a** with 2 equivalents of LA provides further evidence for reaction of the *n*-butyl group (Figure S40). It seems plausible that the presence of Lewis donor LA cleaves the dimeric structure of **2a** into a monomer, although ligand redistribution to form L_2Mg and $n\text{Bu}_2\text{Mg}$ in a complex reaction mixture cannot

be unequivocally ruled out. The addition of 10 equivalents of lactide (vs [Mg]) was subsequently investigated. While the ¹H NMR of this reaction mixture is complex, the diagnostic MgCH_2 resonance of **2a** disappears ($\delta=0.46\text{--}0.54$), providing further evidence to support the initiation of ROP by nucleophilic attack of the *n*-butyl groups.^[22] Furthermore, a distinctive new quartet was observed at $\delta=3.72$ ($^1J_{\text{H-H}}=6.7$ Hz), which is significantly upfield compared to the lactide and poly(lactic acid) methine resonances ($\delta=5.06$, $^1J_{\text{H-H}}=6.7$ Hz and $\delta=5.26\text{--}5.15$ (m), respectively). While the addition of 20 equivalents of lactide (vs [Mg]) generated further PLA, as confirmed by ¹H NMR spectroscopy, the ³¹P NMR resonance remained at constant $\delta=13.9$. These observations provide some support for the notion that the **2a** phosphamidate complex is in the monomeric state during the ROP of LA.

Conclusions

Five new protic phosphamidines **1a-e** have been prepared. For super bulky **1e**, a modified one-pot procedure was developed which expands the range of accessible functional groups on protic phosphamidines and proceeds through a silyl phosphine intermediate. Pro-ligands **1a**, **1c** and **1e** each crystallized in different phosphamidine configurations (Z-syn(N=C), E-syn(P=C) and Z-anti(N=C) respectively), with **1c** also existing as the Z-anti(P=C) and Z-syn(N=C) isomers in the solution-state. Addition of 1 or 0.5 equivalents of $n\text{Bu}_2\text{Mg}$ produced isolable $\text{LMg}n\text{Bu}$ (**2a,b,e**) complexes and thermodynamic sink L_2Mg complexes (**3a-d**). For our heteroleptic examples, the steric profile of the phosphamidine controlled the nuclearity of the complex in the solid and solution state, with dimerization observed for **2a** and **2b**, and a monomeric structure for **2e**. Both the dimeric and monomeric centres retained an accessible metal centre, and **2a**, **2b** and **2e** are all highly active initiators for the ROP of *rac*-LA, converting almost 100 equivalents of monomer within just 2 minutes, and generating polymer chains with $\mathcal{D}=1.02\text{--}1.37$.

With their advantages of both steric and electronic tunability, we have shown that phosphamidine ligands can successfully support highly active main group metal catalysts. To fully capitalize on the advantages and new possibilities enabled by exchanging N for P, we are exploring the preparation of enantiomerically pure phosphamidinate main group complexes and their application into chiral bond-forming transformations.

Supporting Information Summary

The authors have cited additional references within the Supporting Information.^[54–68] Deposition Numbers 2347156 (for **1c**), 2347157 (for **2a**), 2347158 (for **1e**), 2347159 (for **3c**), 2347160 (for **1a**), 2347161 (for **2b**) and 2347162 (for **2e**) contain the supplementary crystallographic data for this paper. These data are provided free of charge by the joint Cambridge

Crystallographic Data Centre and Fachinformationszentrum Karlsruhe <http://www.ccdc.cam.ac.uk/structures>.

Author Contributions

SJU: Conceptualization, investigation (1c, 1e, 2a-e 3a-d, polymerization studies), data curation (synthesis), formal analysis, writing—original draft, review & editing. MWS: Investigation (1a, 1b, 1d). GSN: Investigation and data curation (XRD). JAG: Formal analysis, supervision, writing—original draft, review & editing. MJC: Formal analysis, resources, supervision, writing—original draft, review & editing.

Acknowledgements

The authors thank the European Commission, the EPSRC and the University of Edinburgh for financial support. MWS thanks the Carnegie Trust for the award of a PhD Scholarship, and JAG thanks the British Ramsay Memorial Trust and the UKRI Future Leaders Fellowship (MR/T042710/1). The work was supported by a career integration grant, funded by the FP7 Marie Curie Actions of the European Commission (PCIG14-GA-2013-631483). The authors thank Prof. Michael P. Shaver for access to size exclusion chromatography instrumentation.

Conflict of Interests

The authors declare no conflict of interest.

Data Availability Statement

The data that support the findings of this study are available in the supplementary material of this article.

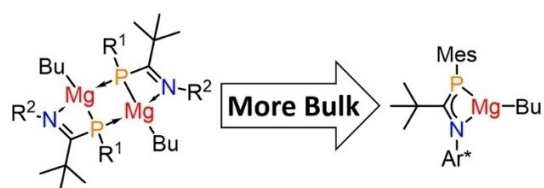
Keywords: Phosphaamidate · Magnesium · Polymerization · Ligand design

- [1] L. C. Wilkins, R. L. Melen, *Coord. Chem. Rev.* **2016**, *324*, 123–139.
- [2] E. Fazekas, P. A. Lowy, M. Abdul Rahman, A. Lykkeberg, Y. Zhou, R. Chambenahalli, J. A. Garden, *Chem. Soc. Rev.* **2022**, *51*, 8793–8814.
- [3] C. Jones, *Nat. Rev. Chem.* **2017**, *1*, 0059.
- [4] D. D. L. Jones, S. Watts, C. Jones, *Inorganics* **2021**, *9*, 72.
- [5] A. J. Boutland, D. Dange, A. Stasch, L. Maron, C. Jones, *Angew. Chem., Int. Ed.* **2016**, *55*, 9239–9243.
- [6] K. Yuvaraj, I. Douair, D. D. L. Jones, L. Maron, C. Jones, *Chem. Sci.* **2020**, *11*, 3516–3522.
- [7] T. X. Gentner, B. Rösch, G. Ballmann, J. Langer, H. Elsen, S. Harder, *Angew. Chem., Int. Ed.* **2019**, *58*, 607–611.
- [8] B. Rösch, T. X. Gentner, J. Langer, C. Färber, J. Eysel, L. Zhao, C. Ding, G. Frenking, S. Harder, *Science* **2021**, *371*, 1125–1128.
- [9] J. D. Masuda, R. T. Boeré, *Dalton Trans.* **2016**, *45*, 2102–2115.
- [10] R. L. Falconer, K. M. Byrne, G. S. Nichol, T. Krämer, M. J. Cowley, *Angew. Chem., Int. Ed.* **2021**, *60*, 24702–24708.
- [11] R. L. Falconer, G. S. Nichol, M. J. Cowley, *Inorg. Chem.* **2019**, *58*, 11439–11448.
- [12] J. D. Masuda, L. Mokhtabad Amrei, R. T. Boeré, *Eur. J. Inorg. Chem.* **2023**, *26*, e202300495.
- [13] R. T. Boeré, M. L. Cole, P. C. Junk, J. D. Masuda, G. Wolmershäuser, *Chem. Commun.* **2004**, 2564–2565.
- [14] T. van Dijk, S. Burck, M. K. Rong, A. J. Rosenthal, M. Nieger, J. C. Sloatweg, K. Lammertsma, *Angew. Chem., Int. Ed.* **2014**, *53*, 9068–9071.
- [15] X. Li, H. Song, C. Cui, *Dalton Trans.* **2009**, 9728–9730.
- [16] K. Issleib, H. Schmidt, H. Meyer, *J. Organomet. Chem.* **1978**, *160*, 47–57.
- [17] M. Westerhausen, M. H. Digeser, W. Schwarz, *Inorg. Chem.* **1997**, *36*, 521–527.
- [18] A. J. Roering, L. T. Elrod, J. K. Pagano, S. L. Guillot, S. M. Chan, J. M. Tanski, R. Waterman, *Dalton Trans.* **2013**, *42*, 1159–1167.
- [19] S. C. Rathnayaka, S. V. Lindeman, N. P. Mankad, *Inorg. Chem.* **2018**, *57*, 9439–9445.
- [20] M. Karplus, *J. Am. Chem. Soc.* **1963**, *85*, 2870–2871.
- [21] M. J. Minch, *Concepts Magn. Reson.* **1994**, *6*, 41–56.
- [22] W. H. Hersh, S. T. Lam, D. J. Moskovic, A. J. Panagiotakis, *J. Org. Chem.* **2012**, *77*, 4968–4979.
- [23] The nitrilium salt was found to be extremely air- and moisture sensitive. Although full conversion was concluded by NMR studies continuous hydrolysis occurred, even with storage in a <0.01 ppm O₂/H₂O glove-box with an argon atmosphere and handling under rigorous inert conditions.
- [24] G. Becker, O. Mundt, M. Rössler, E. Schneider, *Z. Anorg. Allg. Chem.* **1978**, *443*, 42–52.
- [25] W. Uhlig, A. Tzschach, *Z. Anorg. Allg. Chem.* **1989**, *576*, 281–283.
- [26] R. T. Boeré, J. D. Masuda, *Can. J. Chem.* **2002**, *80*, 1607–1617.
- [27] A. Sadique, M. J. Heeg, C. H. Winter, *Inorg. Chem.* **2001**, *40*, 6349–6355.
- [28] G. J. Moxey, F. Ortu, L. Goldney Sidley, H. N. Strandberg, A. J. Blake, W. Lewis, D. L. Kays, *Dalton Trans.* **2014**, *43*, 4838–4846.
- [29] R. J. Schwamm, B. M. Day, N. E. Mansfield, W. Knowelden, P. B. Hitchcock, M. P. Coles, *Dalton Trans.* **2014**, *43*, 14302–14314.
- [30] M. Arrowsmith, B. Maitland, G. Kociok-Köhn, A. Stasch, C. Jones, M. S. Hill, *Inorg. Chem.* **2014**, *53*, 10543.
- [31] M. H. Chisholm, K. Choojun, J. C. Gallucci, P. M. Wambua, *Chem. Sci.* **2012**, *3*, 3445.
- [32] K. Paasch, M. Nieger, E. Niecke, *Angew. Chem., Int. Ed.* **1995**, *34*, 2369–2371.
- [33] L. Falivene, R. Credendino, A. Poater, A. Petta, L. Serra, R. Oliva, V. Scarano, L. Cavallo, *Organometallics* **2016**, *35*, 2286–2293.
- [34] F. H. Allen, D. G. Watson, L. Brammer, A. G. Orpen, R. Taylor, in *International Tables for Crystallography* (Ed: E. Prince), International Union of Crystallography, Chester, England **2006**, pp. 790–811.
- [35] M. H. Chisholm, J. C. Huffman, K. Phomphrai, *J. Chem. Soc., Dalton Trans.* **2001**, 222–224.
- [36] A. P. Dove, V. C. Gibson, P. Hornmiron, E. L. Marshall, J. A. Segal, A. J. P. White, D. J. Williams, *Dalton Trans.* **2003**, 3088–3097.
- [37] L. F. Sánchez-Barba, A. Garcés, M. Fajardo, C. Alonso-Moreno, J. Fernández-Baeza, A. Otero, A. Antiñolo, J. Tejada, A. Lara-Sánchez, M. I. López-Solera, *Organometallics* **2007**, *26*, 6403–6411.
- [38] R. Duan, C. Hu, Z. Sun, X. Pang, X. Chen, *ACS Omega* **2018**, *3*, 11703–11709.
- [39] H. Xie, Z. Mou, B. Liu, P. Li, W. Rong, S. Li, D. Cui, *Organometallics* **2014**, *33*, 722–730.
- [40] Y. Ikada, H. Tsuji, *Macromol. Rapid Commun.* **2000**, *21*, 117–132.
- [41] B. M. Chamberlain, M. Cheng, D. R. Moore, T. M. Ovitt, E. B. Lobkovsky, G. W. Coates, *J. Am. Chem. Soc.* **2001**, *123*, 3229–3238.
- [42] M. H. Chisholm, J. Gallucci, K. Phomphrai, *Inorg. Chem.* **2002**, *41*, 2785–2794.
- [43] M. H. Chisholm, K. Phomphrai, *Inorg. Chim. Acta* **2003**, *350*, 121–125.
- [44] F. E. Kohn, J. W. A. Van Den Berg, V. D. Ridder, *J. Appl. Polym. Sci.* **1984**, *29*, 4265–4277.
- [45] L. F. Sánchez-Barba, A. Garcés, J. Fernández-Baeza, A. Otero, C. Alonso-Moreno, A. Lara-Sánchez, A. M. Rodríguez, *Organometallics* **2011**, *30*, 2775–2789.
- [46] Y. Zhu, C. Romain, V. Poirier, C. K. Williams, *Macromolecules* **2015**, *48*, 2407–2416.
- [47] W. Gruszka, H. Sha, A. Buchard, J. A. Garden, *Catal. Sci. Technol.* **2022**, *12*, 1070–1079.
- [48] M. Cheng, A. B. Attygalle, E. B. Lobkovsky, G. W. Coates, *J. Am. Chem. Soc.* **1999**, *121*, 11583–11584.
- [49] F. Drouin, T. J. J. Whitehorn, F. Schaper, *Dalton Trans.* **2011**, *40*, 1396.
- [50] S. Hosseini, S. O. Martinez-Chapa, *Fundamentals of MALDI-TOF MS Analysis*, Springer, Singapore **2017**.
- [51] T. Chivers, C. Fedorchuk, M. Parvez, *Organometallics* **2005**, *24*, 580–586.
- [52] L. F. Sánchez-Barba, D. L. Hughes, S. M. Humphrey, M. Bochmann, *Organometallics* **2006**, *25*, 1012–1020.

- [53] M. H. Chisholm, *Pure Appl. Chem.* **2010**, *82*, 1647–1662.
- [54] M. Song, B. Donnadiou, M. Soleilhavoup, G. Bertrand, *Chem. Asian J.* **2007**, *2*, 904–908.
- [55] T. Van Dijk, M. K. Rong, J. E. Borger, M. Nieger, J. C. Slootweg, K. Lammertsma, *Organometallics* **2016**, *35*, 827–835.
- [56] Y. Takeda, T. Nishida, S. Minakata, *Chem.-Eur. J.* **2014**, *20*, 10266–10270.
- [57] Y. van den Winkel, H. M. M. Bastiaans, F. Bickelhaupt, *J. Organomet. Chem.* **1991**, *405*, 183–194.
- [58] A. H. Cowley, N. C. Norman, M. Pakulski, G. Becker, M. Layh, E. Kircher, M. Schmidt, *Inorganic Syntheses*, John Wiley & Sons **1990**.
- [59] A. Chartoire, C. Claver, M. Corpet, J. Krinsky, J. Mayen, D. Nelson, S. P. Nolan, I. Peñafiel, R. Woodward, R. E. Meadows, *Org. Process Res. Dev.* **2016**, *20*, 551–557.
- [60] E. W. Y. Wong, A. D. Dange, A. L. Fohlmeister, T. Hadlington, C. Jones, *Aust. J. Chem.* **2013**, *66*, 1144–1154.
- [61] T. M. Ovitt, G. W. Coates, *J. Am. Chem. Soc.* **2002**, *124*, 1316–1326.
- [62] O. V. Dolomanov, L. J. Bourhis, R. J. Gildea, J. A. K. Howard, H. Puschmann, *J. Appl. Crystallogr.* **2009**, *42*, 339–341.
- [63] G. M. Sheldrick, *Acta Cryst.* **2008**, *A64*, 112–122.
- [64] G. M. Sheldrick, *Acta Cryst.* **2015**, *C71*, 3–8.
- [65] Y. Zhao, D. G. Truhlar, *Theor. Chem. Acc.* **2008**, *120*, 215–241.
- [66] M. J. Frisch, G. W. Trucks, H. B. Schlegel, G. E. Scuseria, M. Robb, J. R. Cheeseman, G. Scalmani, V. Barone, G. A. Petersson, H. Nakatsuji, X. Li, G. Caricato, B. Mennucci, H. P. Hratchian, A. F. Izmaylov, J. Bloino, M. H. Zheng, J. L. Sonnenberg, H. M. Ehara, K. Toyota, R. Fukuda, J. Hasegawa, M. Ishida, T. Nakajima, Y. Honda, O. Kitao, E. Nakai, T. Vreven, J. A. Montgomery, Jr., J. E. Peralta, F. Ogliaro, M. Bearpark, J. J. Heyd, V. N. S. Brothers, K. N. Kudin, A. R. Roverov, R. Kobayashi, J. Normand, K. Raghavachari, J. B. J. C. Burant, S. S. Iyengar, J. Tomasi, M. Cossi, N. Rega, J. M. Millam, M. Klene, J. E. Knox, A. J. A. Cross, V. Bakken, C. Adamo, J. Jaramillo, R. Gomperts, R. E. Stratmann, O. Yazyv, J. W. Ochterski, R. L. Martin, K. Morokuma, Ö. Farkas, J. B. Foresman, D. J. Fox, *Gaussian 09, Revision E.01*, Gaussian Inc., Wallingford CT **2009**.
- [67] M. J. Frisch, G. W. Trucks, H. B. Schlegel, G. E. Scuseria, M. A. Robb, J. R. Cheeseman, G. Scalmani, V. Barone, G. A. Petersson, H. Nakatsuji, X. Li, G. Caricato, A. V. Marenich, J. Bloino, B. G. Jenesko, R. Gomperts, B. Mennucci, H. P. Hratchian, J. V. Ortiz, A. F. Izmaylov, J. L. Sonnenberg, D. Williams-Young, F. Ding, F. Lipparini, F. Egidi, J. Goings, B. Peng, A. Petrone, T. Henderson, D. Ranasinghe, V. G. Zakrzewski, J. Gao, N. Rega, G. Zheng, W. Liang, M. Hada, M. Ehara, K. Toyota, R. Fukuda, J. Hasegawa, M. Ishida, T. Nakajima, Y. Honda, O. Kitao, H. Nakai, T. Vreven, K. Throssell, J. A. Montgomery, Jr., J. E. Peralta, F. Ogliaro, M. Bearpark, J. J. Heyd, E. N. Brothers, K. N. Kudin, V. N. Staroverov, T. A. Keith, R. Kobayashi, J. Normand, K. Raghavachari, A. P. Rendell, J. C. Burant, S. S. Iyengar, J. Tomasi, M. Cossi, J. M. Millam, M. Klene, C. Adamo, R. Cammi, J. W. Ochterski, R. L. Martin, K. Morokuma, Ö. Farkas, J. B. Foresman, D. J. Fox, *Gaussian 16, Revision A.03*, Gaussian Inc., Wallingford CT **2016**.
- [68] L. Falivene, Z. Cao, A. Petta, L. Serra, A. Poater, R. Oliva, V. Scarano, L. Cavallo, *Nat. Chem.* **2019**, *11*, 872–879.

Manuscript received: November 11, 2024
Revised manuscript received: November 25, 2024
Version of record online: ■■■, ■■■

RESEARCH ARTICLE



Pushing the limits of phosphoramidate steric bulk, here five new phosphoramidate ligands with systematic R-group variation are reported, along with their homo- and heteroleptic magnesium complexes. The steric

profile of the pendant groups dictates the resultant complex geometry, including an unsolvated three-coordinate magnesium centre. The homoleptic complexes are efficient initiators for *rac*-lactide polymerization.

R group impacts:

- Ligand geometry
- Complex aggregation
- Application

S. J. Urwin*, M. W. Stanford, G. S. Nichol, J. A. Garden*, M. J. Cowley*

1 – 10

Tuneable Phosphaamidate Ligands: Alkyl-Magnesium Complexes Responsive to Increased Ligand Bulk

